

Supporting Information

Enhanced Photoelectrochemical Water Splitting Performance of Molten-salt Carbon Nitride Photoanode with Morphology and Defects Regulation Induced by Hydrochloric Acid Treatment

Xiaochun Li,* Chang Dong, Rouhua Chen, Shimin Jiang, Jiaying Lin, Shaoqi Wu, Sijie Liu, Yuxiu Li, Renping Cao and Bang Lan*

Northeast Guangdong Key Laboratory of New Functional Materials, School of Chemistry and Environment, Jiaying University, Meizhou, 514015, P.R. China

Email: lixiaochun@jyu.edu.cn; jyulb6@163.com

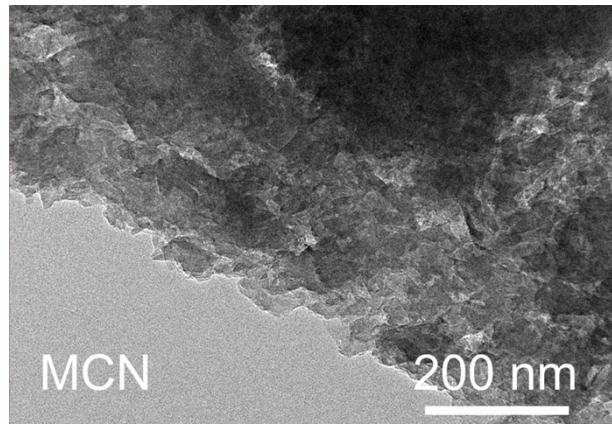


Figure S1. TEM image of the powder sample scraped from MCN films at low magnification.

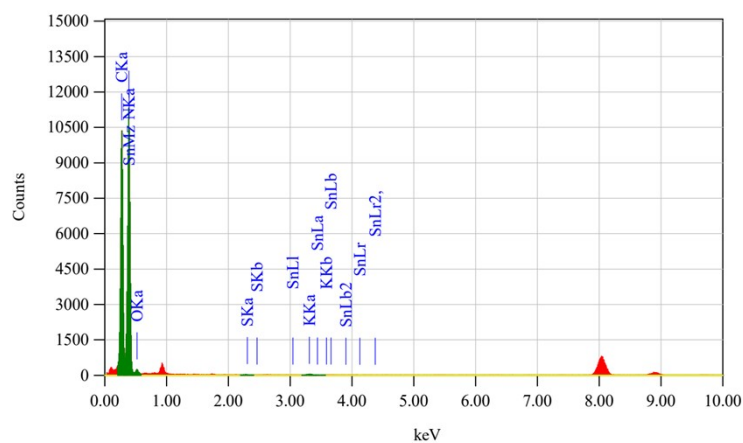


Figure S2. EDS analysis of the powder sample scraped from MCN films accompanied with TEM.

Table. S1. The detail of the elemental analysis of the powder sample scraped from MCN films accompanied with TEM.

Z	Element	Family	(keV)	Mass%	Counts	Sigma	Atom%
6	C	K	0.277	60.36	51409.98	0.20	64.13
7	N	K	0.392	38.82	56221.34	0.17	35.37
8	O	K	0.525	0.54	1086.17	0.02	0.43
11	S	K	2.307	0.03	94.70	0.01	0.01
16	K	K	3.312	0.13	396.10	0.01	0.04
50	Sn	L	3.443	0.12	114.85	0.02	0.01
Total				100.00			100.00

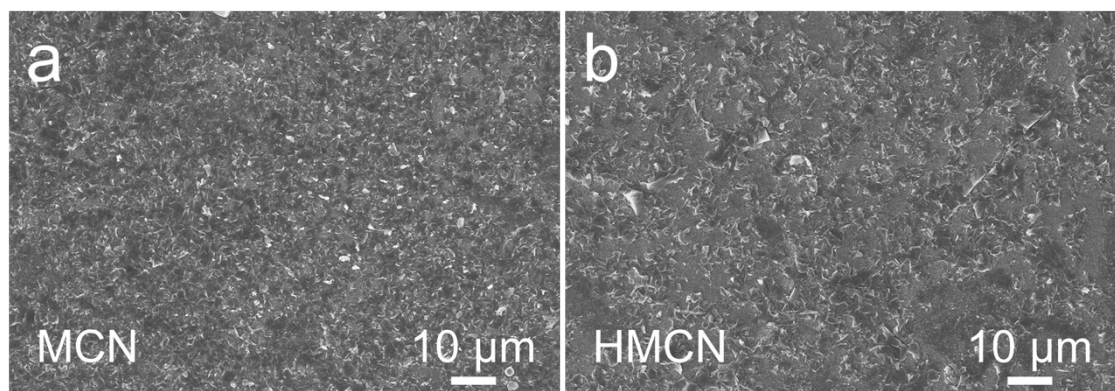


Figure S3. SEM images of (a) MCN and (b) HMCN at low magnification.

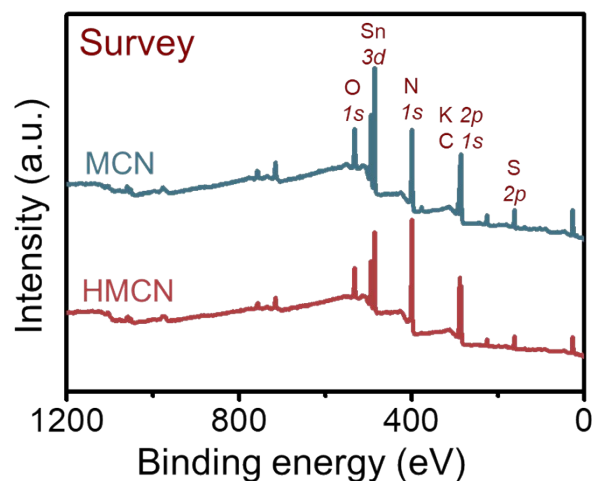


Figure S4. XPS Survey spectra of MCN and HMCN.

Table S2. ICP-OES results for MCN and HMCN.

Sample	Weight (g)	Constant volume (mL)	Element	Element content (mg/L)	Dilution Times	Element content (mg/kg)	Element content (wt%)
MCN	0.0461	10	K	0.4798	1	104.09	0.0104%
HMCN	0.0575	10	K	0.1585	1	27.56	0.0028%

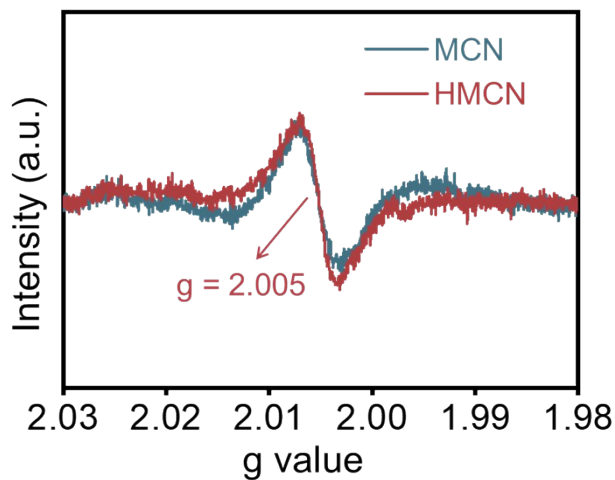


Figure S5. EPR spectra of the powder samples scraped from MCN and HMCN conducted in the dark at room temperature.

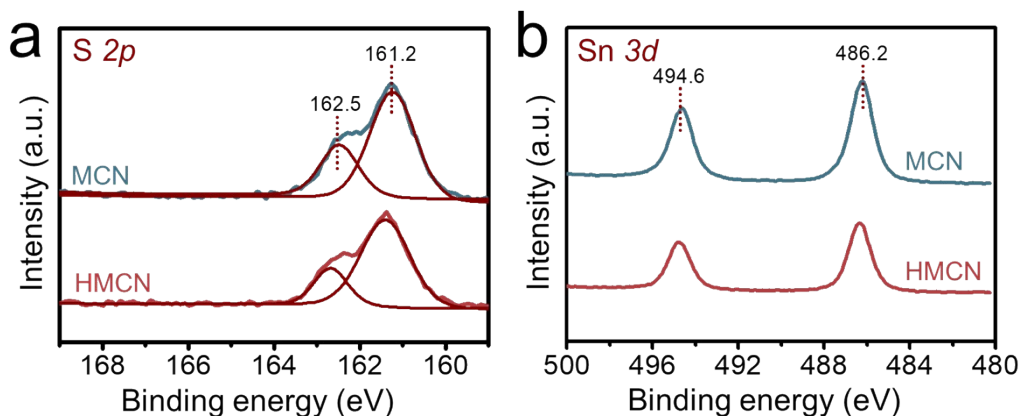


Figure S6. (a) S 2p high-resolution XPS spectra of MCN and HMCN. (b) Sn 3d high-resolution XPS spectra of MCN and HMCN.



Figure S7. The digital photograph of MCN and HMCN.

Table S3. Summary of PEC performance of this work and the reported PCN-based photoanodes.

Catalyst	Preparation method	Photocurrent density ($\mu\text{A cm}^{-2}$)	Potential vs. RHE (V)	Electrolyte	Light source	Corresponding Author (Ref.)
HMCN	Post-treatment	ca. 233	1.23	1.0 M NaOH (pH ~ 14)	100 mW cm^{-2} AM 1.5G 300 W Xe lamp	This work
CN _{TUB} photoanode	<i>In situ</i> synthesis	870	1.23	0.1 M KOH (pH ~ 14)	100 mW cm^{-2} AM 1.5G (Newport)	¹
g-CN/SnS ₂ composite film	<i>In situ</i> synthesis	844.6	1.23	0.2 M Na ₂ SO ₄ (pH ~ 7)	100 mW cm^{-2} AM 1.5G (Newport)	²
K-PHI photoanode	<i>In situ</i> synthesis	ca. 800	1.23	1.0 M NaOH (pH ~ 14)	100 mW cm^{-2} AM 1.5G (Newport)	³
PCN photoanode	<i>In situ</i> synthesis	650	1.23	0.1 M KOH (pH ~ 14)	100 mW cm^{-2} AM 1.5G 300 W Xe lamp	⁴
CN-MR/NiFeO _x H _y electrode	Post-treatment	472 ± 10	1.23	0.1 M KOH (pH ~ 14)	100 mW cm^{-2} , AM 1.5G (Newport)	⁵
CN _{TM} photoanode	<i>In situ</i> synthesis	353	1.23	0.1 M KOH (pH ~ 14)	100 mW cm^{-2} AM 1.5G (Newport)	⁶
CN _{NaN} photoanode	<i>In situ</i> synthesis	343	1.23	1.0 M NaOH (pH ~ 14)	100 mW cm^{-2} AM 1.5G 300 W Xe lamp	⁷
CN-MSG _{0.75} /M photoanode	<i>In situ</i> synthesis	270	1.23	0.1 M KOH (pH ~ 14)	100 mW cm^{-2} AM 1.5G (Newport)	⁸
DPCN photoanode	<i>In situ</i> synthesis	242	1.23	0.5 M H ₂ SO ₄ (pH ~ 1)	100 mW cm^{-2} AM 1.5G 150 W Xe lamp	⁹
CNP films	<i>In situ</i> synthesis	230	1.23	0.5 M Na ₂ SO ₄ (pH ~ 7)	100 mW cm^{-2} AM 1.5G Xe lamp	¹⁰
CN films	<i>In situ</i> synthesis	228.2	1.23	0.2 M Na ₂ SO ₄ (pH ~ 7)	100 mW cm^{-2} AM 1.5G (Newport)	¹¹
2CSCN films	<i>In situ</i> synthesis	200	1.23	1.0 M NaOH (pH ~ 14)	100 mW cm^{-2} AM 1.5G (Newport)	¹²

KPCN	<i>In situ</i> synthesis	ca. 162	1.23	1.0 M NaOH (pH ~ 14)	100 mW cm ⁻² AM 1.5G 300 W Xe lamp	13
P/B-layer-doping C ₃ N ₄ photoanode	<i>In situ</i> synthesis	150 ± 10	1.23	0.1 M Na ₂ SO ₄ (pH ~ 7)	100 mW cm ⁻² AM 1.5G 300 W Xe lamp	14
CN-MeM/M _{0.20}	<i>In situ</i> synthesis	133	1.23	0.1 M KOH (pH ~ 14)	100 mW cm ⁻² AM 1.5G (Newport)	15
<i>In situ</i> grown porous CN/rGO films	<i>In situ</i> synthesis	124.5	1.23	0.1 M KOH (pH ~ 14)	100 mW cm ⁻² AM 1.5G (Newport)	16
g-CN PNR array photoanode	<i>In situ</i> synthesis	120.5	1.23	0.1 M Na ₂ SO ₄ (pH ~ 7)	100 mW cm ⁻² AM 1.5G 500 W Xe lamp	17
5p-PCN films	<i>In situ</i> synthesis	ca. 120	1.23	1.0 M NaOH (pH ~ 14)	100 mW cm ⁻² AM 1.5G (Newport)	18
phosphorylated PCN films	Post-treatment	ca. 120	1.23	1.0 M NaOH (pH ~ 14)	100 mW cm ⁻² AM 1.5G (Newport)	19
SOCN-75 films	<i>In situ</i> synthesis	119.2	1.23	0.1 M Na ₂ SO ₄ (pH ~ 7)	100 mW cm ⁻² AM 1.5G (Newport)	20
CN films	<i>In situ</i> synthesis	116	1.23	0.1 M KOH (pH ~ 14)	100 mW cm ⁻² AM 1.5G (Newport)	21
PCN photoanode	<i>In situ</i> synthesis	ca. 110	1.23	1.0 M NaOH (pH ~ 14)	100 mW cm ⁻² AM 1.5G (Newport)	22
CN-U ₁₀ M _{0.5} photoelectrode	<i>In situ</i> synthesis	ca. 110	1.23	0.1 M KOH (pH ~ 14)	100 mW cm ⁻² AM 1.5G (Newport)	23
Boron-doped CN films	<i>In situ</i> synthesis	103.2	1.23	0.1 M Na ₂ SO ₄ (pH ~ 7)	100 mW cm ⁻² AM 1.5G 150 W Xe lamp	24
PCN films	<i>In situ</i> synthesis	100	1.23	1.0 M NaOH (pH ~ 14)	100 mW cm ⁻² AM 1.5G (Newport)	25

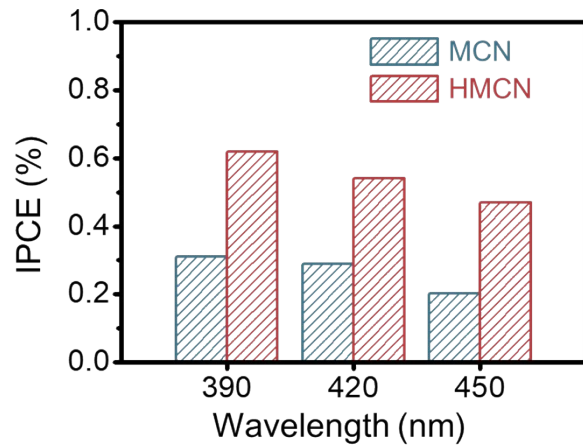


Figure S8. IPCE measurements of MCN and HMCN.

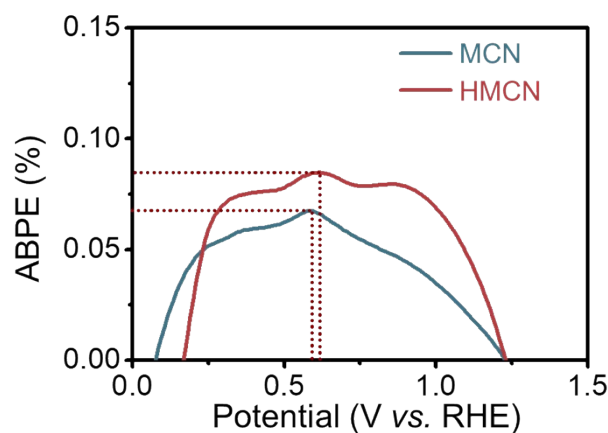


Figure S9. ABPE curves of MCN and HMCN calculated from LSV curves.

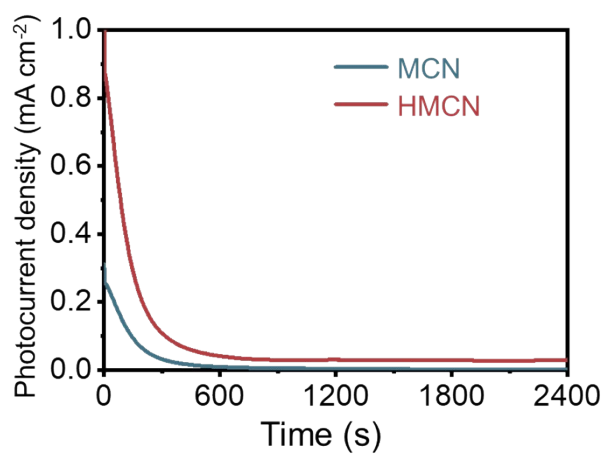


Figure S10. Stability measurements of MCN and HMCN at 1.23 V vs. RHE in 1.0 M NaOH aqueous solution under AM 1.5G illumination.

Table S4. Fitted parameters for electrochemical impedance spectroscopy results.

Samples	R_s (Ω)	R_{trap} (Ω)	C_{bulk} (F)	$R_{ct, ss}$ (Ω)	C_{ss} (F)
MCN light	5.76	11.01	108.9×10^{-5}	3132	8.46×10^{-5}
HMCN light	18.08	17.79	1.14×10^{-5}	386.7	7.93×10^{-5}

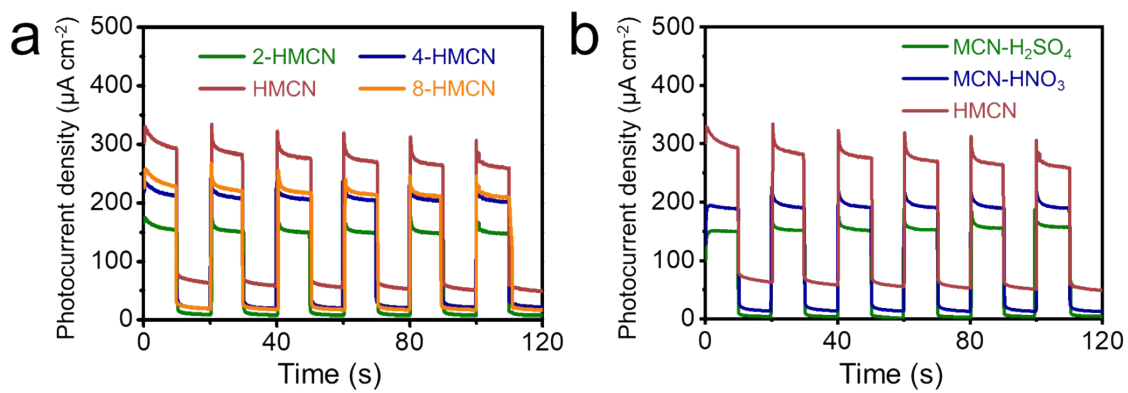


Figure S11. (a) Photocurrent densities of x-HMCN at 1.23 V vs. RHE under AM 1.5G illumination. (b) Photocurrent densities of the samples prepared using an identical procedure as HMCN but with 6 M H_2SO_4 or 6 M HNO_3 at 1.23 V vs. RHE under AM 1.5G illumination.

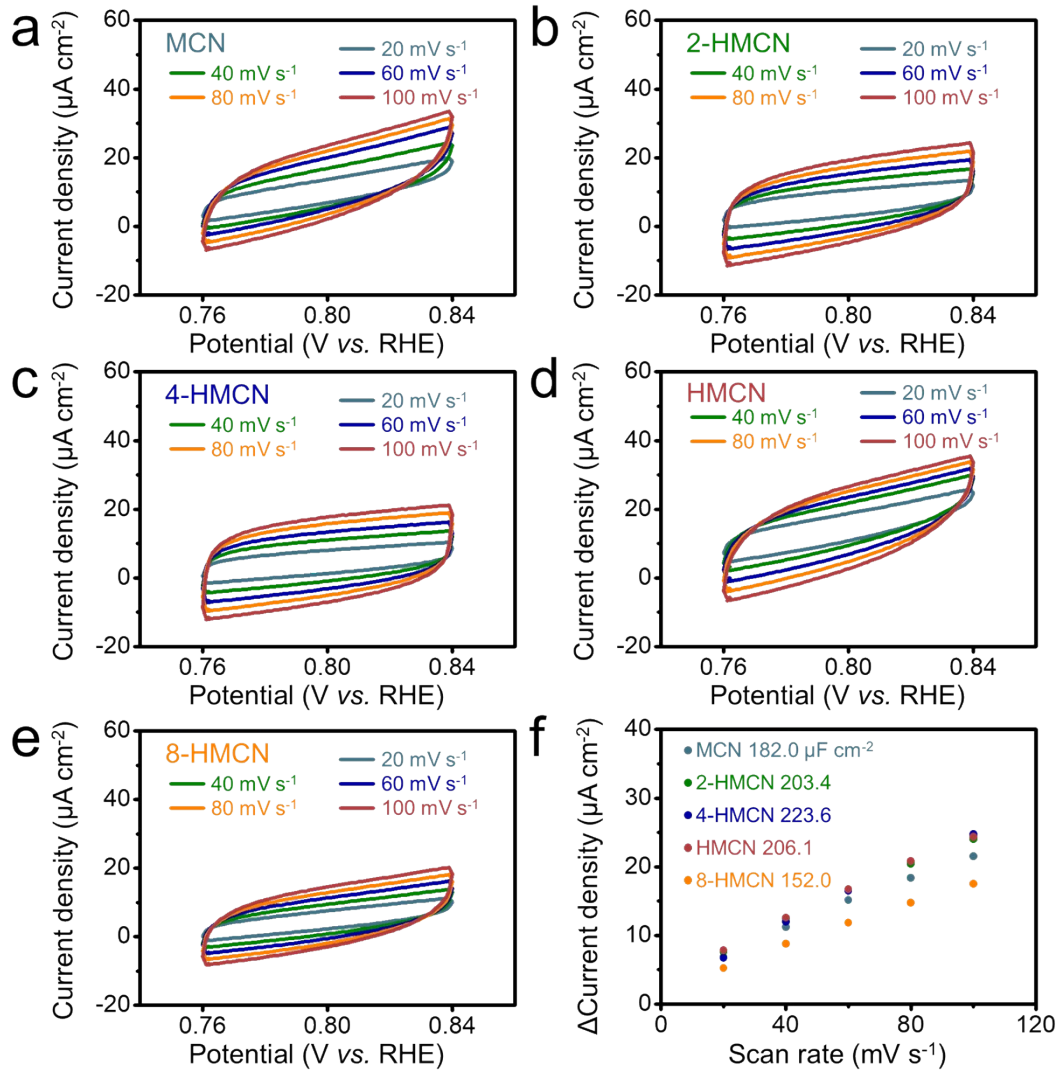


Figure S12. Cyclic voltammetry curves of (a) MCN, (b) 2-HMCN, (c) 4-HMCN, (d) HMCN and (e) 8-HMCN in the region of 0.76~0.84 V vs. RHE under dark. (d) The differences in current density variation at 0.80 V vs. RHE plotted against scan rates fitted to a linear regression for x-HMCN.

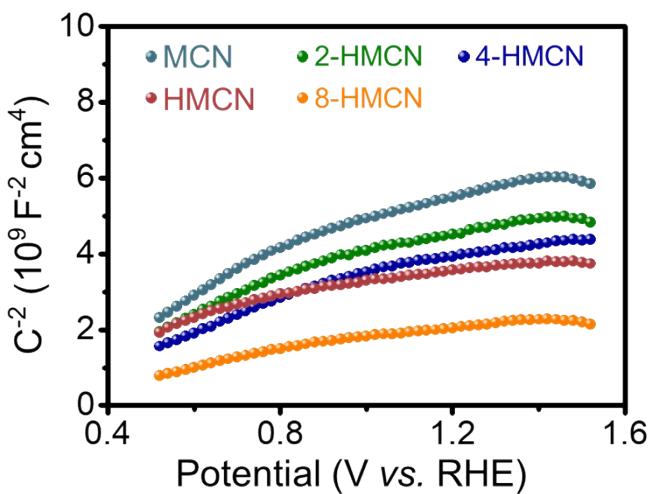


Figure S13. Mott-Schottky plots of MCN and x -HMCN at 1000 Hz without illumination.



Figure S14. The band structure diagrams of MCN and HMCN.

References

1. T. Shmila, S. Mondal, S. Barzilai, N. Karjule, M. Volokh and M. Shalom, *Small*, 2023, **19**, 2303602.
2. W. Xiong, H. Wang, Z. Wang, F. Huang, T. Dudka, Z. Lu, Y. Zhao and R.-Q. Zhang, *J Mater. Chem. A*, 2020, **8**, 12767-12773.
3. X. Li, X. Chen, Y. Fang, W. Lin, Y. Hou, M. Anpo, X. Fu and X. Wang, *Chem. Sci.*, 2022, **13**, 7541-7551.
4. J. Zhang, J. Zhang, C. Dong, Y. Xia, L. Jiang, G. Wang, R. Wang and J. Chen, *Small*, 2023, **19**, 2208049.

-
5. N. Karjule, C. Singh, J. Barrio, J. Tzadikov, I. Liberman, M. Volokh, E. Palomares, I. Hod and M. Shalom, *Adv. Funct. Mater.*, 2021, **31**, 2101724.
6. J. Qin, J. Barrio, G. Peng, J. Tzadikov, L. Abisdris, M. Volokh and M. Shalom, *Nat. Commun.*, 2020, **11**, 4701.
7. X. Li, W. Wu, Y. Zhuang, W. Song, T. Guo, R. Chen, J. Duan, S. Liu, B. Lan and R. Cao, *Int. J. Hydrogen Energ.*, 2025, **105**, 1340-1347.
8. N. Karjule, J. Barrio, L. Xing, M. Volokh and M. Shalom, *Nano Lett.*, 2020, **20**, 4618-4624.
9. X. Fan, Z. Wang, T. Lin, D. Du, M. Xiao, P. Chen, S. A. Monny, H. Huang, M. Lyu, M. Lu and L. Wang, *Angew. Chem. Int. Ed.*, 2022, **61**, e202204407.
10. Q. Jia, S. Zhang, Z. Gao, P. Yang and Q. Gu, *Catal. Sci. Technol.*, 2019, **9**, 425-435.
11. W. Xiong, S. Chen, M. Huang, Z. Wang, Z. Lu and R. Q. Zhang, *Chemsuschem*, 2018, **11**, 2497-2501.
12. X. Li, J. Wang, J. Xia, Y. Fang, Y. Hou, X. Fu, M. Shalom and X. Wang, *Chemsuschem*, 2022, **15**, e202200330.
13. X. Li, D. Zheng, W. Wu, X. Long, B. Yang, X. Huang, J. Duan, S. Liu, B. Lan and R. Cao, *New J. Chem.*, 2024, **48**, 19452-19461.
14. P. Luan, Q. Meng, J. Wu, Q. Li, X. Zhang, Y. Zhang, L. A. O'Dell, S. R. Raga, J. Pringle, J. C. Griffith, C. Sun, U. Bach and J. Zhang, *Chemsuschem*, 2020, **13**, 328-333.
15. J. Xia, N. Karjule, L. Abisdris, M. Volokh and M. Shalom, *Chem. Mater.*, 2020, **32**, 5845-5853.
16. G. Peng, J. Qin, M. Volokh, C. Liu and M. Shalom, *J Mater. Chem. A*, 2019, **7**, 11718-11723.
17. B. Guo, L. Tian, W. Xie, A. Batool, G. Xie, Q. Xiang, S. U. Jan, R. Boddula and J. R. Gong, *Nano Lett.*, 2018, **18**, 5954-5960.
18. X. Li, Z. Cheng, Y. Fang, X. Fu and X. Wang, *Sol. RRL*, 2020, **4**, 2000168.
19. Y. Fang, X. Li and X. Wang, *Chemsuschem*, 2019, **12**, 2605-2608.
20. M. Huang, H. Wang, W. Li, Y.-L. Zhao and R.-Q. Zhang, *J Mater. Chem. A*, 2020, **8**, 24005-24012.
21. G. Peng, J. Albero, H. Garcia and M. Shalom, *Angew. Chem. Int. Ed.*, 2018, **57**, 15807-15811.
22. Y. Fang, X. Li, Y. Wang, C. Giordano and X. Wang, *Appl. Catal. B*, 2020, **268**, 118398.
23. A. Tashakory, N. Karjule, L. Abisdris, M. Volokh and M. Shalom, *Adv. Sustain. Syst.*, 2021, **5**, 2100005.
24. Q. Ruan, W. Luo, J. Xie, Y. Wang, X. Liu, Z. Bai, C. J. Carmalt and J. Tang, *Angew. Chem. Int. Ed.*, 2017, **56**, 8221-8225.
25. Y. Fang, X. Li and X. Wang, *ACS Catal.*, 2018, **8**, 8774-8780.